FIRST OPERATION OF THE LANL/AES NORMAL CONDUCTING RADIO FREQUENCY PHOTOINJECTOR*

N.A. Moody#, D.C. Nguyen, H.L. Andrews, G.O. Bolme, L.J. Castellano, C.E. Heath, F.L. Krawczyk, S.I. Kwon, D.C. Lizon, F.A. Martinez, P. Marroquin, M. Prokop, R.M. Renneke, P.L. Roybal, W.T. Roybal, P.A. Torrez, W.M. Tuzel, and T.J. Zaugg
Los Alamos National Laboratory, Los Alamos, NM 87544, U.S.A.

Abstract

The LANL/AES normal-conducting radio-frequency (NCRF) injector has undergone high power testing, confirming field gradients of up to 10 MV/m at the cathode. Most NCRF designs are limited to low-duty-factor operation to constrain rf power consumption and limit ohmic heat generation. This cavity structure utilizes high density micro-channel cooling to successfully remove heat with the option of dynamic temperature control to actively adjust cavity resonance. This first high power rf test demonstrated stable cw (100% duty cycle) operation using resonant frequency tracking and produced intentional dark current emission from a roughened cathode blank. Resulting end-point x-ray measurements confirm the cathode gradient of 9.8 ± 0.2 MV/m required for acceleration of nC bunches to a beam energy of 2.5 MeV.

INTRODUCTION

The response of the accelerator community to the successes of the 4th generation UV/x-ray light source has been formidable, resulting in a number of proposed high brightness schemes. High-brightness injectors use picosecond laser pulses in phase with an rf accelerating field to produce and rapidly accelerate short electron bunches to relativistic energies [1]. The combination of high accelerating gradients and magnetic solenoid emittance compensation reduce emittance growth due to space charge and rf effects [2].

Recent efforts in injector development, including the LANL/AES efforts described herein, have been focused on maximizing the cathode accelerating gradients while increasing the duty factor [3]. High-duty operation requires improvements that enable vacuum compatibility with semiconductor photocathodes and relatively low (<15MV/m) gradients to limit ohmic heating on the rf surfaces, but still high enough to launch nC bunch charge with good emittance.

These needs motivated development of the LANL/AES injector. Figure 1 shows an exploded view of the gun, together with its bucking and focusing solenoids which provide the required focusing, emittance compensation, and zero field at the cathode. As a 2.5-cell, π-mode, 700 MHz room temperature gun, it has field gradients of 7, 7, and 5 MV/m, respectively, in each the first three cells. The fourth cell shown is a vacuum plenum providing unprecedented pumping capacity of up to 600 l/s.

*Work supported by Office of Naval Research (ONR)
#nmoody@lanl.gov

EXPERIMENTAL SETUP

Initial Testing

Before installation began, a rough leak check verified the vacuum integrity of the structure prior to any further testing. When not under vacuum, the structure remained under positive pressure of dry argon.

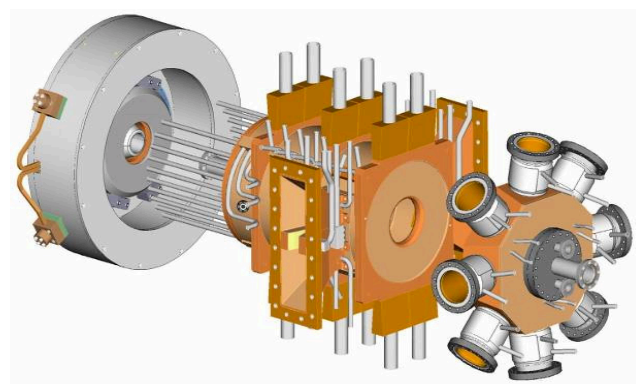

Figure 1: Layout of NCRF injector.

Typical UHV cleanroom practices were strictly followed when working on either the injector itself or any of its subcomponents. Approximate flow rates of each of the cooling channels was also measured and compared to design specifications, showing good agreement.

Vacuum System Configuration

Significant attention was given to vacuum preparation because additional stages of this project intend to utilize an alkali-based photocathode, whose lifetime strongly depends upon the cleanliness of its surrounding environment. Combined diode, star-cell ion, and non-evaporable getter (NEG) pumping [4] has brought the vacuum level at the cathode to 5×10^{-10} Torr following a system bake and pressure in the vacuum cell is near the lower detection limit of all installed ion gauges.

Vacuum Bakeout

To remove adsorbed gases and other impurities from fabrication, a two-step thermal bakeout of the injector was performed. The photoinjector and its auxiliary vacuum components were wrapped in heater tape and divided into 12 temperature zones. Each zone was controlled using an Omega 9000A temperature control module with redundant control thermocouples. The system was heated first to 175°C during a primary bake and then to 150°C during a secondary process.

LOW POWER RF TESTS

Bead Pull Measurements

A bead-pull setup was used to scan a metal bead along the cavity axis. During low power rf excitation at 700 MHz, it displaces electromagnetic energy, causing a frequency shift proportional to the square of the electric field level at the position of the bead. A phase lock loop was used to continuously adjust the frequency to maintain resonance during a run that consisted of about 400 data points. The electric fields were then calculated from the measured frequency shifts in the code Quadplot [4]. In this code, the calculated electric fields were also compared to the theoretical fields from the Superfish model and were shown to be within 7% agreement with both pre-braze measurements and design calculations.

Cavity Q Measurements

For the unloaded (Q_0) measurement, antennas were inserted for on-axis electric coupling: one mounted on the cathode flange and the other at the beam exit flange of the unexcited fourth vacuum cell. The probes consisted of ¼" copper rods which were sequentially shortened in increments of 1/8" until the loaded Q did not change with additional reduction in antenna length. This guaranteed that the presence of the probes was not loading the cavity. From the measured loaded Q and the corrections for the coupling βs of the ridge loaded waveguide [5], Q_0 has been determined to be reasonably close to the expected value from the Superfish simulations. The experimentally determined Q_0 value thus determined was 29,108 at a center frequency of 700.2 MHz while the Superfish simulation predicted a Q_0 of 32,600 at 700.35 MHz.

RF Pickup Loop Coupling

Magnetically coupled pickup loops were installed on cells 2 and 3, as shown in Figure 2. They were positioned such that the final attenuation was -60dB [5].

HIGH POWER OPERATION

RF power for cavity testing was provided by a previously reported MW-class klystron system [6] which was integrated into a control system based on the EPICS architecture.

Cavity Conditioning

The first step toward high power operation was systematic conditioning of the rf window, the couplers, and the surfaces inside the main cavity volume. This was accomplished by using a combination of rf pulse and ramping formats on the klystron drive whilst closely monitoring changes in pressure at the locations of the rf window/coupler and vacuum pumping cell.

Multipacting was observed at distinct regions cavity pickup loop powers near 120 and 380 mW especially. Slowly increasing rf power throughout the conditioning phase, followed by sequential periods of operation at very low power, enabled eventual operation at observed pickup loop power of 702 mW.

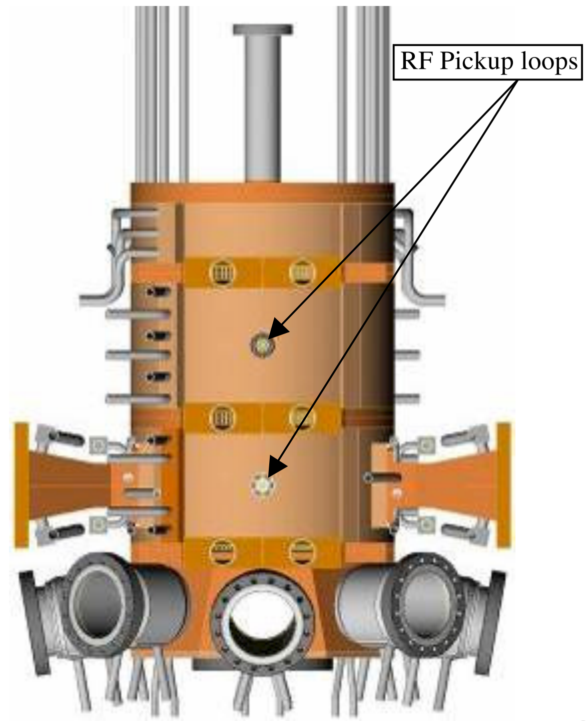

Figure 2: Location of pickup loops in cells 2 and 3.

End-Point X-ray Measurements

Accelerated field emission electrons impinged on a stainless steel flange and the resulting bremsstrahlung photons were detected 9 meters downstream of the photoinjector by a high-purity germanium photon detector. Detected signals were conditioned using a Tennelec spectroscopy amplifier for pulse height analysis and the pulse height was converted and stored by analog-to-digital converter module interfaced to a data acquisition workstation.

With added collimators and absorbers, the photon count rates were kept below the maximum count rate of 6,000 s^{-1} at cavity pickup power up to 600 mW. Above 600 mW pickup loop power, the count rate exceeded 12,000 s^{-1} but reasonable end-point energies could still be extrapolated in spite of double-photon events at the high energy end of the photon spectrum. The time interval was chosen such that the number of counts provided good statistics to establish an accurate reading of the end-point energy.

The end-point energies at low rf power are directly read from the photon energy where the photon count, N_{ph}, is reduced to one. The error in the number of photon count is $(N_{ph})^{0.5}$ so the signal-to-noise ratio is also 1 when $N_{ph} = 1$, corresponding to the limit of detection in photon counting. By reading and averaging the end-point energies at $N_{ph} = 1$, we obtain the end-point energy for a given power level. As can be seen in Figure 3, corresponding to 250 mW of cavity pickup loop power, the data points at $N_{ph} = 1$ have a mean value of 1,449 keV and standard deviation of 69 keV. The PARMELA predicted end-point energy is 1,416 keV, demonstrating excellent agreement with experiment.

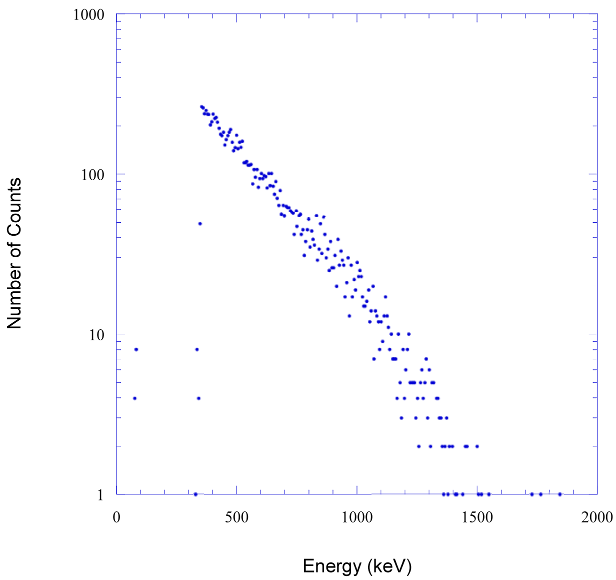

Figure 3: X-ray photon counts at cavity pickup loop power 250 mW.

Recall that the above data corresponds to relatively low power in the cavity. At higher power, end-point energies must be observed at the transitions from single-photon to double-photon events [7]. The end-point energies using this method of differentiation are plotted, together with PARMELA predicted end-points, versus cavity power in Figure 4.

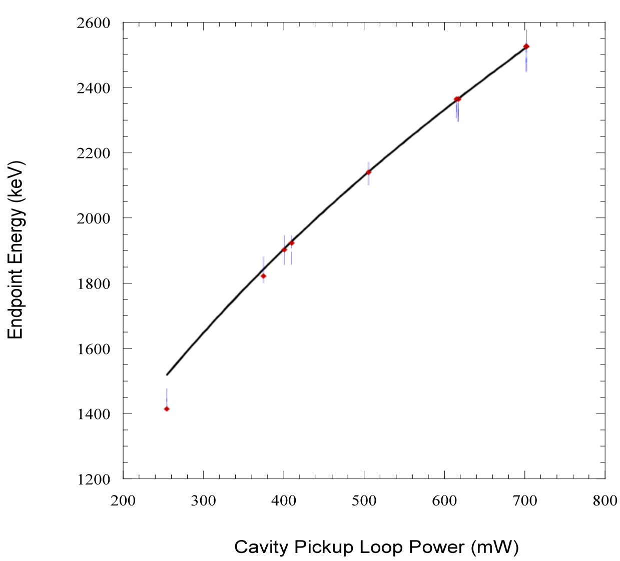

Figure 4. End-point photon energy versus cavity power.

Vertical bars in Figure 4 are measured data ± 2 standard deviations, the circles are PARMELA prediction, and the line is analytic calculation.

Both the measured and PARMELA-predicted end-point energies agree over the entire range of rf power. Also plotted is a curve of end-point energies analytically calculated using $E_{max}=(3.0\text{MeV})(P_{cav})^{0.5}$, where P_{cav} is cavity pickup loop power normalized to 1 watt. Thus, the analytic and PARMELA predictions agree well with nearly all experimental data.

CONCLUSION

We report the first cw operation of a normal-conducting rf injector at cathode gradients up to 9.8 ± 0.2 MV/m. These gradients are adequate for accelerating nC bunches to beam energies of 2.5 MeV with an expected normalized rms emittance of 2.75 μm for bunch of 1 nC.

Field emission was observed experimentally and also simulated with PARMELA at different cavity power levels to predict the maximum electron energies at each power level. The measured end-point energies are in excellent agreement with PARMELA predictions using the accelerating gradients deduced from the measured cavity pickup loop power.

ACKNOWLEDGMENTS

We appreciate the financial support from the Office of Naval Research and the High Energy Laser Joint Technology Office. We also thank Lloyd Young for modifying the PARMELA code to model field emission in the NCRF injector.

REFERENCES

[1] Hernandez-Garcia, *et al*. (2008), Physics Today 61 (2): 44-49.

[2] B.E. Carlsten, Nucl. Instr. Meth. Phys. Res. A 285 (1989) 313.

[3] R. Akre, *et al.*, Phys. Rev. Spec. Topics Accel. Beams, 11 (2008) 030703.

[4] K. Kishiyama, *et al.,* "Testing of Vacuum Pumps for the APT/LEDA RFQ," Proceedings of the LINAC98, Chicago (1998), Paper TU4095.

[5] F. Krawczyk, *et al.*, "Initial rf measurements of the cw normal-conducting rf injector," Proceedings of the LINAC08, Victoria, BC, Canada (2008), Paper TUP18.

[6] W.T. Roybal, *et al.*, "A 700 MHz, 1 MW cw rf system for a FEL 100 mA rf injector," Proc. of 2005 Particle Accelerator Conference, pp. 2413, Knoxville, TN (2005).

[7] D.C. Nguyen, N.A. Moody, *et al*. (2011). Phys. Rev. Spec. Topics Accel. Beams 14(3): 030704.